

**Unidirectional Water Transport on a Two-dimensional Hydrophilic Channel with
Anisotropic Superhydrophobic Barriers**

Qier An^a, Jinshu Wang,^{b} Feng Zhao,^c Peiliu Li^d and Lei Wang^{e*}*

a School of Aviation, Inner Mongolia University of Technology, 49 Aimin Street, Xincheng District, Hohhot, Inner Mongolia 010051, Inner Mongolia, P. R. China.

b Key Laboratory of Advanced Functional Materials of Education Ministry of China, School of Materials Science and Engineering, Beijing University of Technology, 100 Pingleyuan, Chaoyang District, Beijing 100124, Beijing, P. R. China.

c Hainan Vocational University of Science and Technology, Haikou 571126, China

d Biomechanics and Biomaterials Laboratory, Department of Applied Mechanics, School of Aerospace Engineering, Beijing Institute of Technology, Beijing 100081, PR China

e Beijing Key Laboratory of Cryo-Biomedical Engineering, CAS Key Laboratory of Cryogenics, Technical Institute of Physics and Chemistry, Chinese Academy of Sciences, Beijing 100190, P. R. China.

Electronic Supplementary Material (ESI) for Soft Matter.

Supplementary Figure Legends: (Figure S1-S10)

Supplementary Table : (Table S1-S3)

Movie : (Movie 1-6)

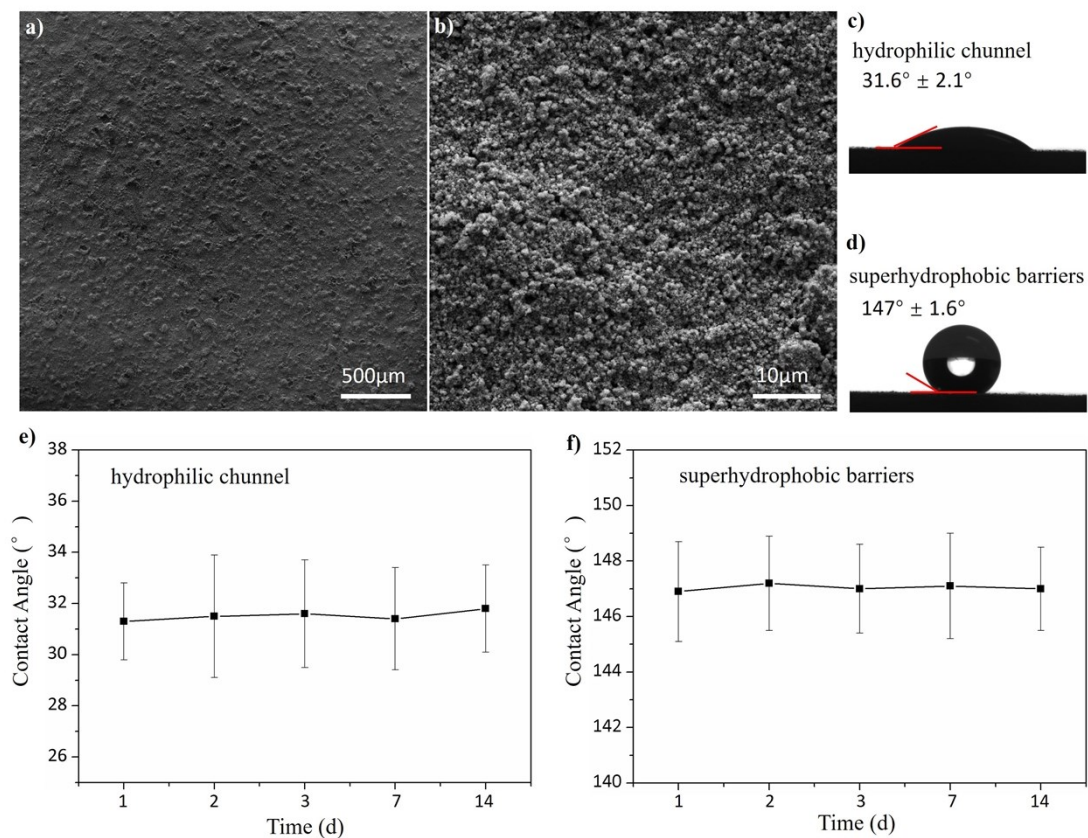


Fig. S1. a-b) SEM images of the surface, where the glass slice is covered by the TiO_2 particles with a diameter of 500 nm to 1 μm . c) The contact angle of the hydrophilic channel is $31.6 \pm 2.1^\circ$. d) The contact angle of superhydrophobic barriers is $147 \pm 1.6^\circ$. e) The change in the contact angle of the hydrophilic channel in 14 days. f) The change in the contact angle of superhydrophobic barriers is 14 days.

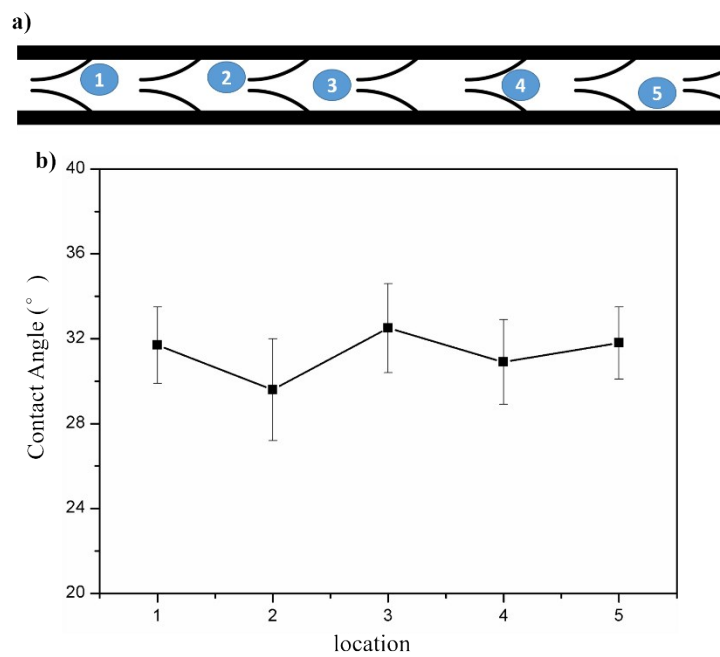


Fig. S2. a) Schematic shows the selection of test locations. b) Test results of contact angle for each location.

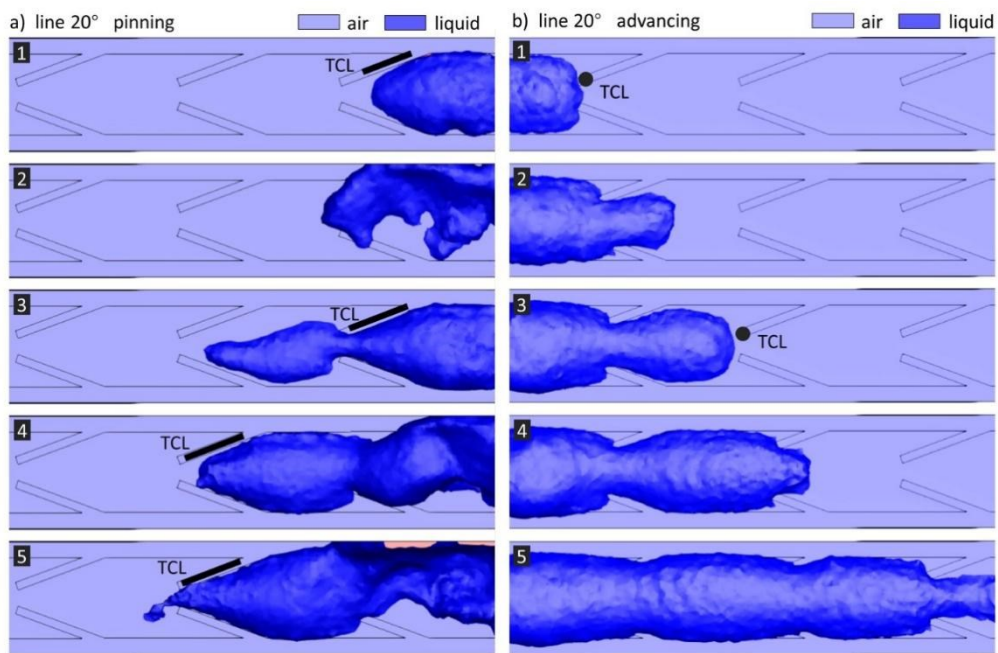


Fig. S3. The simulations of line 20° . a) Water blockage phenomenon on the pinning side, where water spills out of the channel when they cross the barriers. b) Water blockage phenomenon on the advancing side, where liquid cross the barrier and rapidly moves forward into the next joint.

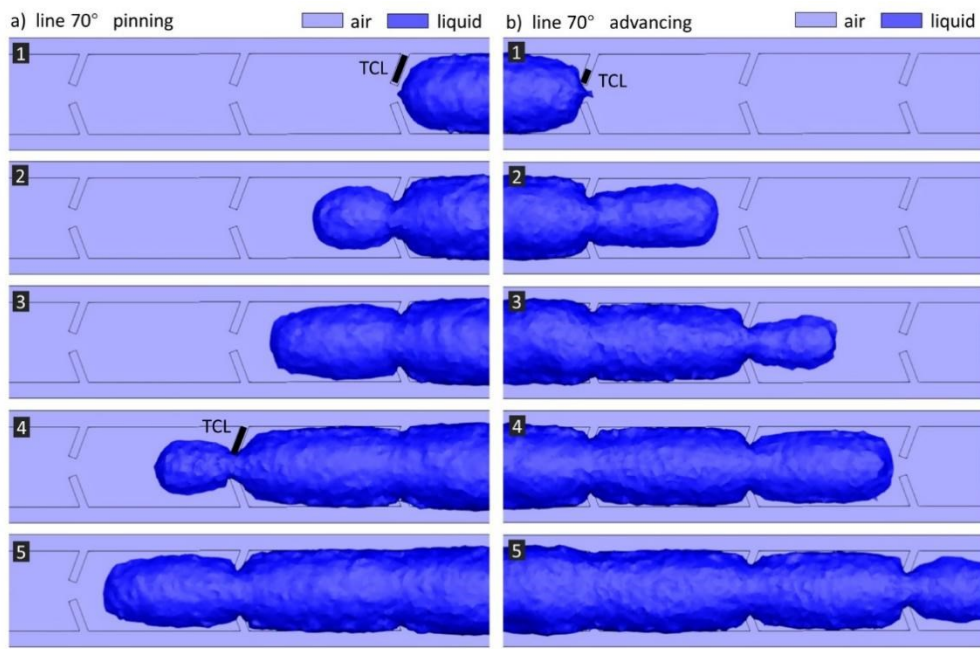


Fig. S4. The simulations of line 70° . a) Water blockage phenomenon on the pinning side, where water flows across the barriers. b) Water blockage phenomenon on the advancing side, where liquid crosses the barrier and rapidly moves forward into the next joint.

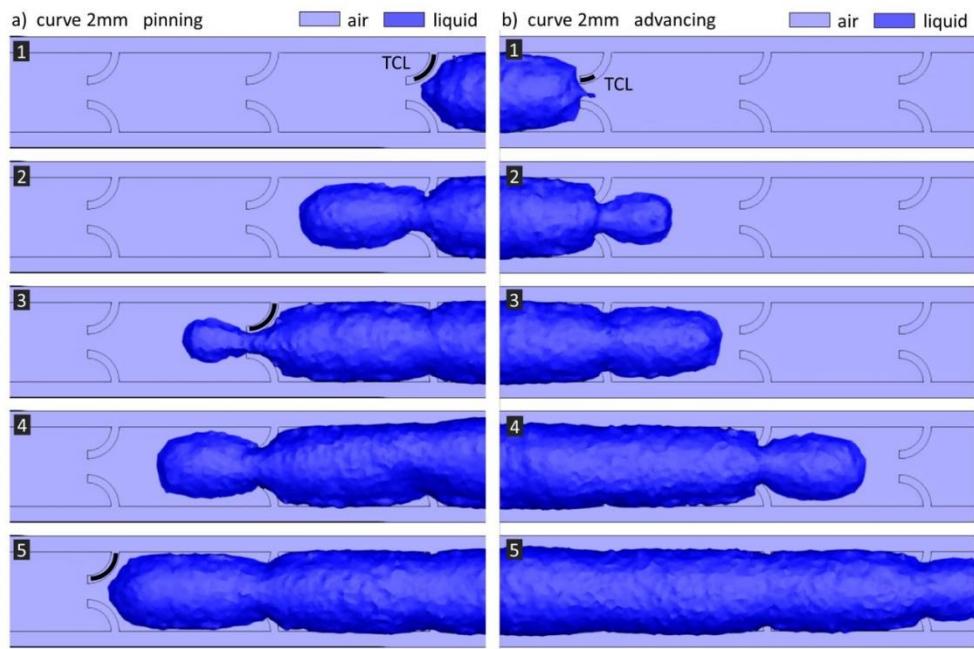


Fig. S5. The simulations of curve 2 mm. a) Water blockage phenomenon on the pinning side, where water can flow across the barriers. b) Water blockage phenomenon on the advancing side, where liquid goes across the barrier and rapidly moves forward into the next joint.

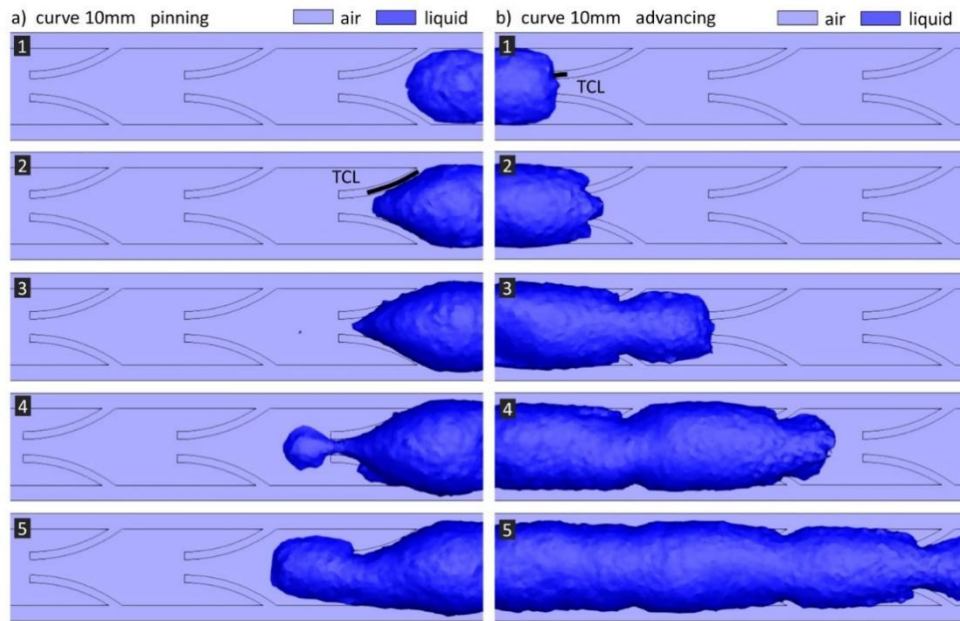


Fig. S6. The simulations of curve 10 mm. a) Water blockage phenomenon on the pinning side, where water spills out of the channel when they cross the barriers. b) Water blockage phenomenon on the advancing side, where liquid cross the barrier and rapidly moves forward into the next joint.

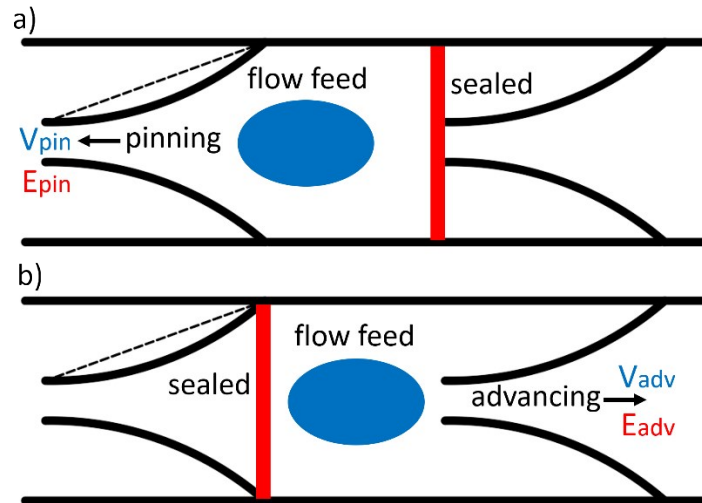


Fig. S7. a) The advancing side is sealed; V_{pin} and E_{pin} are the volumes and total energy of injected water when it passes into the pinning side. b) The pinning side is sealed; V_{adv} and E_{adv} are the volumes and total energy of the injected water when it passes into the advancing side.

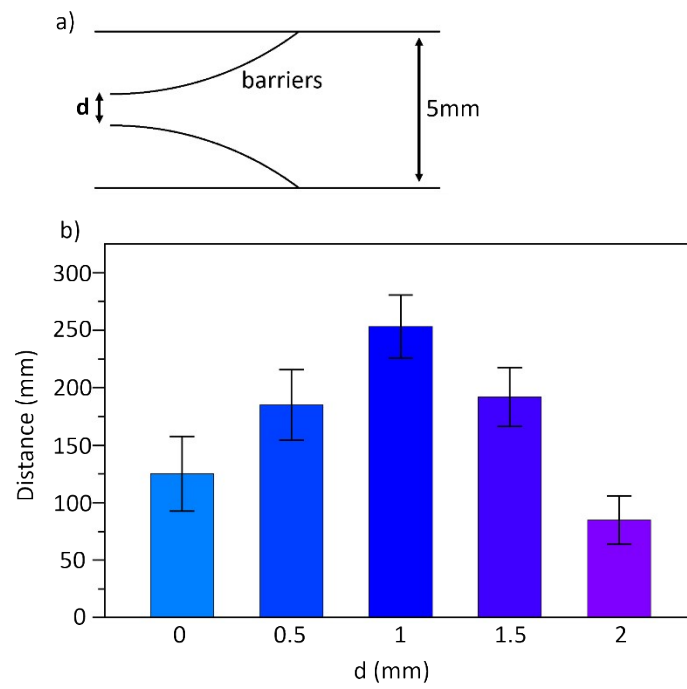


Fig. S8. a) Schematic of curve 10 mm and d . b) The relationship between the distance of unidirectional fluid transport and d .

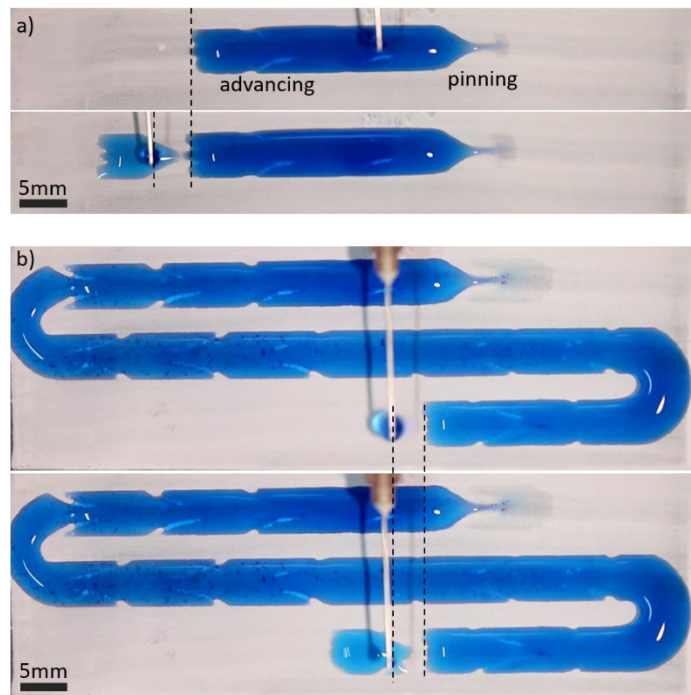


Fig. S9. The discontinuous water charging process demonstrates the consistency of the the directionality of water spreading in each joint of the channel.

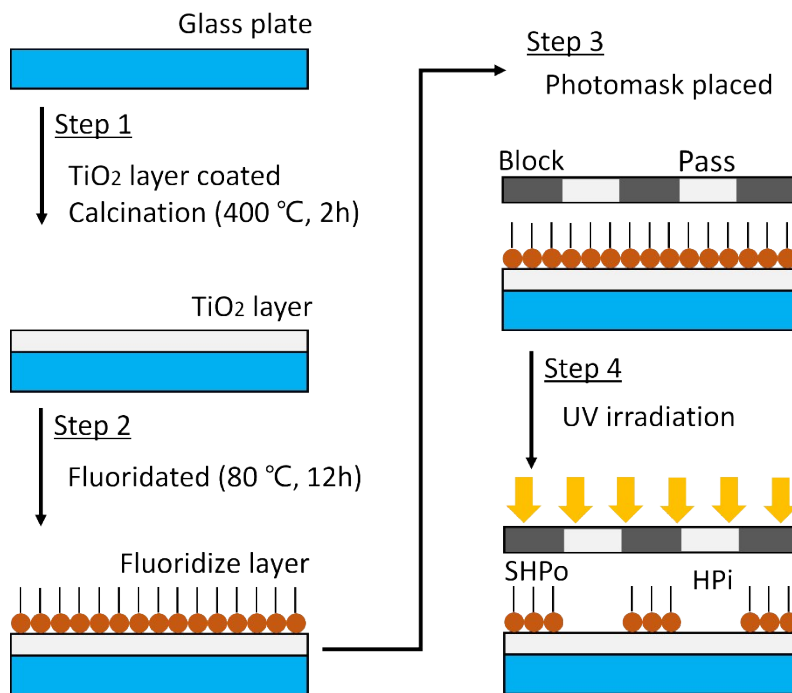


Fig. S10. Fabrication of two-dimensional titanium dioxide (TiO₂) based hydrophilic surface with anisotropic superhydrophobic barriers.

Supplementary Table Legends: (Table S1-S3)

Table S1. The distance and volume of unidirectional fluid transport, E_{pin}/E_{adv} of curve barriers with higher R.

	E_{pin}/E_{adv}	Distance (mm)	Volume (μ L)
curve R=10mm	1.32	276	2236
curve R=15mm	1.25	249	2159
curve R=20mm	1.16	235	2112

Table S2. The distance of unidirectional fluid transport of curve 10 mm with different scale size and flow velocity.

Distance (mm)		Scale (%); Channel width (mm)			
		100; 5	80; 4	60; 3	40; 2
Rate of flow ($\mu\text{L/s}$)	50	276 \pm 42	205 \pm 40	113 \pm 38	32 \pm 15
	25	296 \pm 51	279 \pm 44	198 \pm 35	125 \pm 32
	10	301 \pm 49	295 \pm 42	267 \pm 48	255 \pm 46

Table S3. Parameters

Surface tension	0.072 N/m
Gravitational acceleration	9.8 m/s ²
Liquid density	998.2 kg/m ³
Liquid viscosity	0.001003 kg/ms
Gas density	1.225 kg/m ³
Gas viscosity	1.7894×10 ⁻⁵ kg/ms
Contact angle	147 deg/30 deg
Flow rate	50 μL/s